Supplementary Material

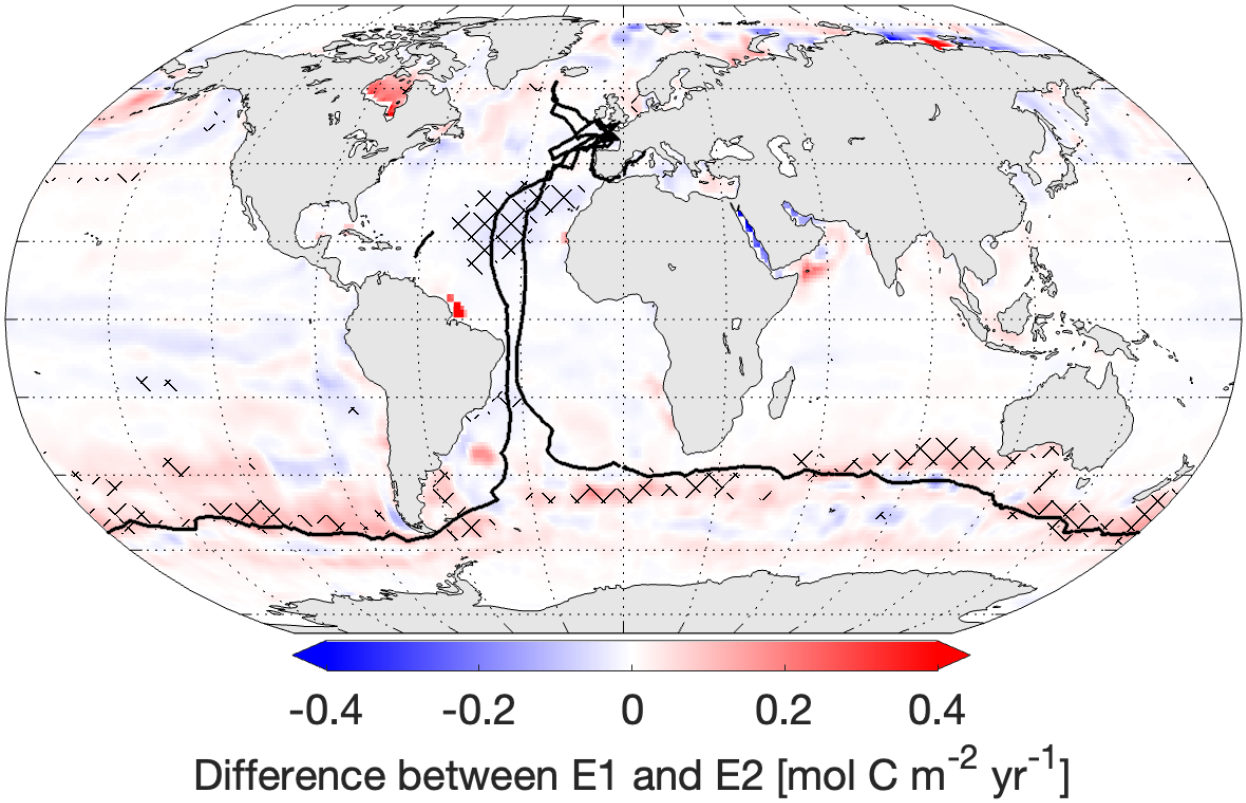

Figure 1: Difference between the air-sea CO_2 fluxes in ensemble E1 (based on SOCATv2022 including Seaexplorer data) and in ensemble E2 (based on SOCATv2022 excluding Seaexplorer data) averaged over 2018 - 2021*. Hatching indicates significant differences. Blue indicates increased carbon uptake due to the addition of Seaexplorer data, red indicates reduced carbon uptake due to the addition of Seaexplorer data. Black lines represent sailboat tracks from 2018 - 2021. Figure generated using a mapping package for MATLAB*[32].

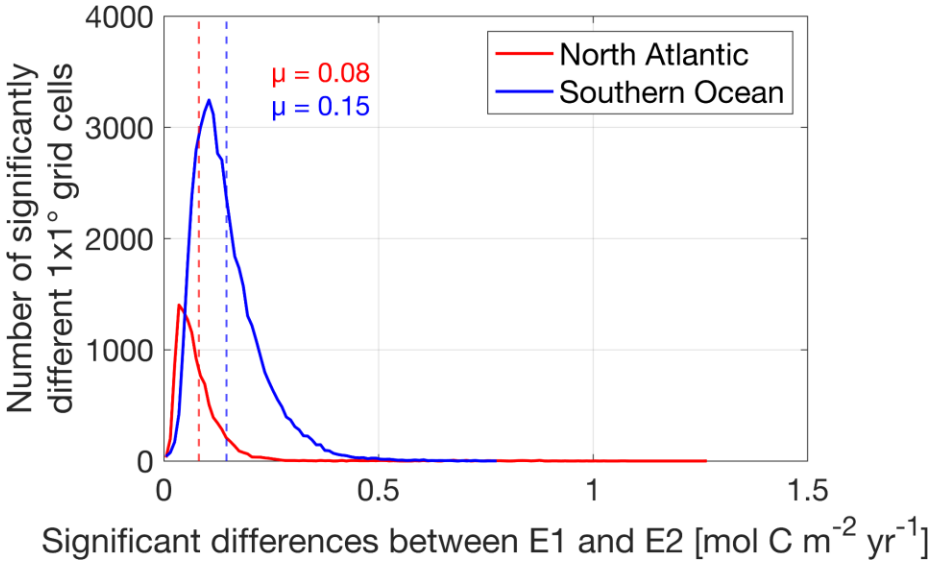

Figure 2: Histogram of the absolute magnitude of significant differences between the air-sea CO_2 flux E1 (based on SOCATv2022 including Seaexplorer data) and the air-sea CO_2 flux E2 (based on SOCATv2022 excluding Seaexplorer data) in the Southern Ocean and the North Atlantic.

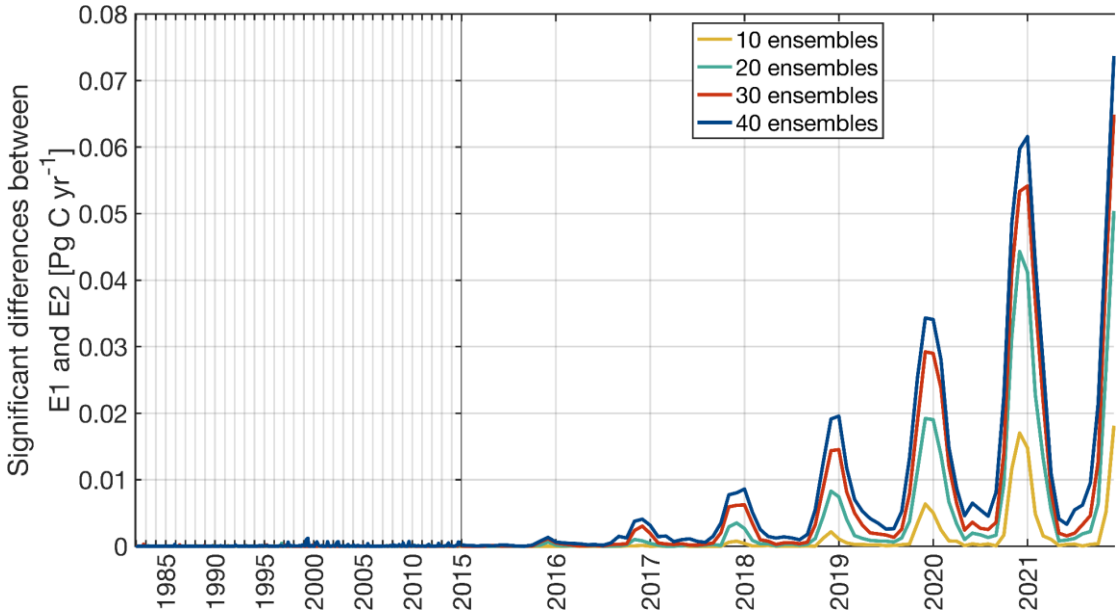

Figure 3: Time series of the magnitude of significant differences between the air-sea CO_2 fluxes E1 and E2 (including and excluding sailboat pCO_2 data) based on the ensemble size of flux reconstructions. Changes in the magnitude of significant

differences decrease with an increasing number of flux reconstructions as the random uncertainty is less well constrained.

Tab. 1: Integrated flux bias in Pg C yr $^{-1}$ in 2021

	Due to missing Seaexplorer data (comparison E1 and E2)	Due to random measurement uncertainty (comparison E1 and E3)	Due to fixed measurement bias (comparison E1 and E4)
Global	0.04	0.01	- 0.06
North Atlantic	0.00	0.00	- 0.01
Southern Ocean	0.05	0.02	- 0.03

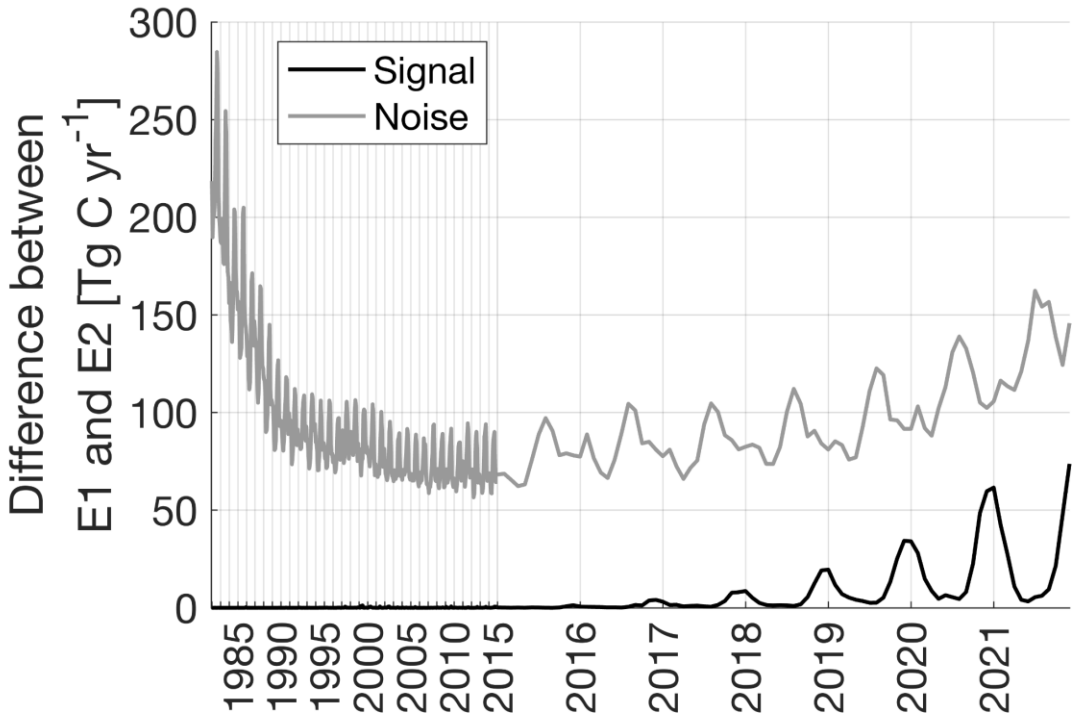

Figure 4: Temporal development of signal and noise.